Status and Results of the OECD Benchmark Exercise on TMI-2 Plant

G. BANDINI [1], S. WEBER [2], H. AUSTREGESILO [2], P. DRAI [3], M. BUCK [4], M. BARNAK [5], P. MATEJOVIC [5], H. MUSCHER [6], F. KRETZSCHMAR [6], M. HOFFMANN [7], L. SALLUS [8] J. BULLE [8], H. G. LELE [9], B. CHATTERJEE [9] , K. DOLGANOV [10], A. KAPUSTIN [10], D. TOMASHCHIK [10], P. GROUDEV [11], A. STEFANOVA [11], R. GENCHEVA [11], A. AMRI [12]

[1] ENEA, Bologna (IT) [2] GRS, Garching (GE) [3] IRSN, Cadarache (FR)
[4] IKE, Stuttgart (GE) [5] IVS, Trnava (SK) [6] KIT, Karlsruhe (GE)
[7] RUB, Bochum (GE) [8] Tractebel Engineering, Brussels (BE)
[9] BARC, Mumbai (IN) [10] IBRAE-RAS, Moscow (RU) [11] INRNE, Sofia (BUL)
[12] OECD-NEA, Paris (FR)

ABSTRACT

The OECD benchmark exercise on TMI-2 plant was launched by the Working Group on the Analysis and Management of Accidents (WGAMA) of OECD/CSNI, in conjunction with the WP 5.4 "Corium and Debris Coolability – Bringing Research Results into Reactor Applications" of the EU/SARNET2 network of excellence. The main objective of this benchmark exercise is to investigate the ability of current advanced codes to predict in-vessel core melt progression and degraded core coolability by the analysis of different severe accident sequences, and comparing the various results from several computer codes. The planned work foresees the simulation of three representative severe accident sequences addressing core reflooding issue, starting from different degrees of core degradation, and molten core slumping into the lower plenum. Two accident sequences have been simulated in the time frame of SARNET2 activities. These first two accident sequences concern a small break loss of coolant accident (SBLOCA) and a surge line break (SLB) in station blackout (SBO) conditions. Both accident sequences were first analysed without high pressure injection until almost complete core melting, corium slumping and possible vessel failure. In a second step, core reflooding is simulated by start-up of high pressure injection at different time instants, corresponding to a pre-defined amount of core degraded materials. In this paper the code result comparison regarding the analysis of SBLOCA and SLB accident sequences and related reflooding scenarios is presented and discussed. Eleven organizations from eight countries are participating in this benchmark exercise using five different codes.

1 INTRODUCTION

Based on the conclusions of the previous OECD benchmark exercise on alternative TMI-2 scenario [1], a new benchmark exercise on TMI-2 plant was launched by the Working Group on the Analysis and Management of Accidents (WGAMA) of OECD/CSNI, in conjunction with the WP 5.4 "Corium and Debris Coolability – Bringing Research Results into Reactor Applications" of the EU/SARNET2 network of excellence.

The present benchmark aimed at examining different severe accident sequences involving safety system operation failure and various severe accident management (SAM) measures, e.g. depressurization, delayed start of high pressure injection (HPI), loss of auxiliary feed water (AFW), etc. The impact on hydrogen production, core coolability, corium relocation into the lower plenum and vessel failure had to be examined. This benchmark should contribute in establishing some consensus on how the deemed confidence on the codes can be established and on what technical ground. It should also establish a basis for the future work (e.g., uncertainty analysis, sensitivity analysis) in relation with important aspects of in-vessel melt pool retention.

The work foresees the simulation of three representative severe accident sequences addressing core reflooding issue, starting from different degrees of core degradation, and molten core slumping into the lower plenum. The work started in February 2011 and the end of the benchmark activities is foreseen by February 2014.

Two accident sequences have been simulated in the time frame of the SARNET2 activities, thus by March 2013. These sequences concern a small break loss of coolant accident (SBLOCA) and a surge line break (SLB) accident under station blackout (SBO) conditions. Both were first analysed without high pressure injection until almost complete core melting, corium slumping and possible vessel failure. In a second step, core reflooding was simulated by start-up of high pressure injection at different instants, corresponding to a pre-defined amount of core degraded materials. The comparison between code results regarding the analysis of SBLOCA and SLB accident sequences, including reflooding scenarios, is presented hereafter.

2 PARTICIPANTS AND CODES

The list of participants as well as the list of used computer codes is given in Table I. Several research organizations involved in the SARNET2 WP5.4 contributed to the benchmark activities using different computer codes. All participants were SARNET2 partners except IBRAE-RAS from Russia. Both mechanistic and integral codes have been used in the analysis.

Table I: participants and codes

Participant	Country	Code
GRS	Germany	ATHLET-CD Mod 2.2 Cycle B
IKE		ATHLET-CD V2.2C
KIT		ASTEC V2.0R2p2 and MELCOR 1.8.6
RUB		ATHLET-CD V2.2A
ENEA	Italy	ASTEC V2.0R2p2
IRSN	France	ICARE/CATHARE V2.3rev1
IVS	Slovak Republic	ASTEC V2.0R2p2
INRNE	Bulgaria	ASTEC V2.0R2p2
Tractebel Engineering	Belgium	MELCOR 1.8.6
BARC	India	ASTEC V2.0R2p2
IBRAE-RAS	Russia	SOCRAT V3

3 ANALYSIS OF SEVERE ACCIDENT SEQUENCES

After the definition of a common steady-state for the TMI-2 plant, the main results of the first two analysed SBLOCA and SBO accident sequences are presented. For both sequences, a base case without reflooding has been analysed in a first step, with core degradation progression towards molten corium relocation in the lower plenum and eventual vessel failure. In a second step, the impact of reflooding on core degradation and hydrogen generation has been investigated starting the reflooding from different core degradation conditions. Two reflooding scenarios have been taken into account for both sequences starting from a pre-defined total amount of degraded core materials: 10 tons and 45 tons.

3.1 TMI-2 steady-state at nominal power

The steady-state condition of TMI-2 plant at nominal power has been defined according to the final specifications of MSLB Benchmark [2], trying to achieve the best agreement on the plant state at the beginning of the calculated transient, in particular regarding the total coolant mass in the primary system. The range of calculated values of main steady-state plant parameters is compared with TMI-2 plant data in Table II. In general, the deviations from the reference plant data are limited and considered acceptable. In particular, the maximum deviation of total primary mass is below 1.3%. The agreement on this parameter is very important because of its impact on the timing of primary pump stop which dictates the beginning of core uncovery for the SBLOCA sequence. The largest deviations are evidenced on pressurizer level and steam generator (SG) steam temperature and feed water flow rate, but they are not expected to produce significant deviations on the calculated transient evolution.

Table II: main steady-state plant parameters

Parameter	Unit	Calculated values (range)	TMI-2 plant data
Reactor core power	MW	2772	2772
Pressurizer pressure	MPa	14.82 - 15.15	14.96
Hot leg temperature	K	589.3 - 594.8	591.15
Cold leg temperature	K	560.3 - 565.7	564.15
Primary loop flow rate	kg/s	8472 - 8888	8800
Pressurizer collapsed level	m	5.05 - 5.94	5.588
Total primary mass	kg	219830 - 225650	222808
SG secondary pressure	MPa	6.41 - 6.55	6.41
SG steam temperature	K	564.7 - 588.3	572.15
SG feed water flow rate	kg/s	701.8 - 791.0	761.1

3.2 SBLOCA sequence

The initial event of the SBLOCA accident scenario is a small break of 20 cm^2 size in the hot leg of loop A with a simultaneous total loss of the main feed water at t = 0 s. As soon as the break opens, the primary pressure begins to decrease. After few tens of seconds, the fast SG dry-out with consequent loss of heat removal from the primary side results in sudden primary pressure increase. The opening of the pressurizer operated relief valve (PORV) cannot prevent the primary pressure rise and, therefore, reactor scram occurs when the pressurizer pressure set-point of 16.3 MPa is exceeded.

The auxiliary feed water starts at t = 100 s trying to restore the water in the SG up to 1 m level in a time interval of 100 s. Afterwards the SG level is maintained constant by controlling the auxiliary feed water flow rate. At the same time the SG pressure is increased up to 7.0 MPa and then maintained at this value throughout the remaining transient.

In the base case calculation without reflooding, the postulated failure of the HPI and low pressure injection (LPI) systems induces the uncompensated loss of primary coolant inventory towards core uncovery, which leads to severe accident conditions. A constant make-up flow rate of 3 kg/s is performed in the cold leg during the whole transient, while there is no letdown flow simulated, in order to reduce the uncertainty in the calculation regarding the boundary conditions with the primary system. The primary pumps are

stopped on the basis of primary coolant inventory depletion when the primary mass falls below 85 tons. In the base case the accidental transient is let free to evolve towards core uncovery, heat-up, melting and relocation into the lower plenum, until possible lower head vessel failure.

3.2.1 Base case without reflooding

The aspects relevant to plant thermal-hydraulic behaviour are illustrated in Figures 1 to 3. The break mass flow rate calculated by the participants is compared in Figure 1. The break mass flow rate decreases quickly at the beginning of the transient according with the decreasing primary pressure, until saturation conditions are reached in equilibrium with the secondary pressure at about t = 300 s. Then the break flow rate (liquid and steam mixture) continues to progressively decrease due to increasing void fraction at the break. After primary pumps stop around t = 2300 s with consequent hot leg draining, the break flow rate switches from mixture to pure steam flow and then suddenly reduces by about 60%. From this point onwards, the break flow rate decrease is consistent with the primary pressure behaviour. All codes are able to reproduce the above described break flow rate behaviour and then the agreement among all calculations is very good. The good agreement in the calculation of the break flow rate leads to similar agreement in the calculated primary mass (Figure 1).

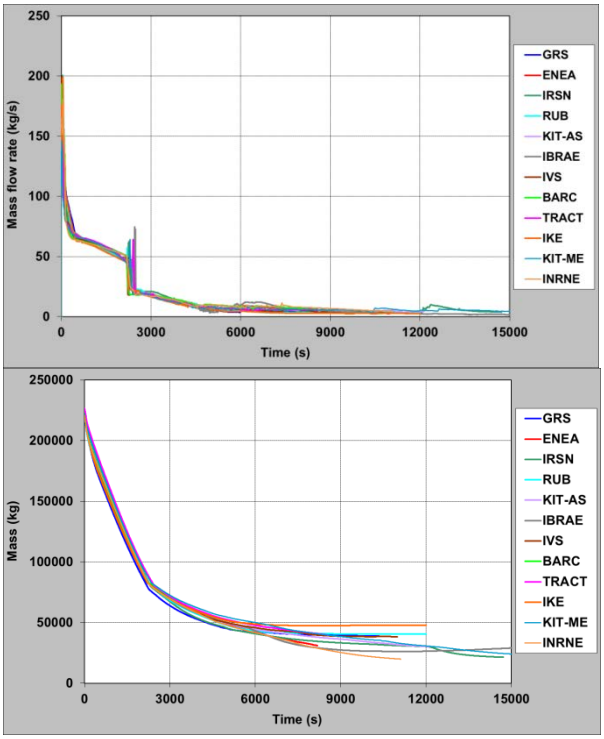

Figure 1: break flow rate (left) and total primary mass (right)

The timing of primary pumps stop is almost coincident in all calculations (see Figure 2). There is a significant spread in the calculated primary mass flow rates before pump stop likely due to different pump characteristic curves used. After primary pumps stop and consequent hot leg draining, the core decay heat removal by the secondary side progressively reduces down to zero, since there is no natural convection in the primary loops. Therefore, the primary pressure (Figure 2) is no more sustained by the steam generator pressure and then tends to progressively reduce. Some significant deviations are observed on the calculated primary pressure during the core uncovery and heat-up phase from t = 3000 s onwards. Several pressure spikes occurred in most of the calculations and they are consistent with the timing of molten material slumping into the lower plenum and consequent strong water vaporization. The largest pressure peaks are calculated by IVS,

IRSN, IBRAE-RAS, Tractebel Engineering and KIT-MELCOR as a consequence of molten jet break-up with enhanced thermal interaction between water and molten material. In other ASTEC calculations than the one by IVS, the jet fragmentation during slumping was not taken into account (model choice). The lowest primary pressure until t = 12000 s is calculated by RUB since no core slumping is modelled with the version 2.2A of ATHLET-CD used.

The time evolution of the core collapsed water level is compared in Figure 3. The collapsed water level reduces before primary pumps stop due to core void fraction increase. Just after the stop of primary pumps the water level suddenly increases, owing to stratification of liquid water in the lowest volumes of the primary circuit, including the vessel. This behaviour is predicted by most of the participants and codes. Afterwards the water level behaviour is in quite good agreement among all calculations. Noticeable water level fluctuations are calculated from t = 4400 s onwards when molten material slumping into the lower plenum occurs; first the water level suddenly increases due to upwards displacement of water by the relocated material and then the water level reduces following strong water vaporization in the lower plenum. In some cases, the water level in the vessel reduces below the bottom of the core during the core slumping phase, because of molten jet fragmentation and strong thermal interaction with water (IRSN, IBRAE-RAS, IVS, Tractebel Engineering and KIT-MELCOR).

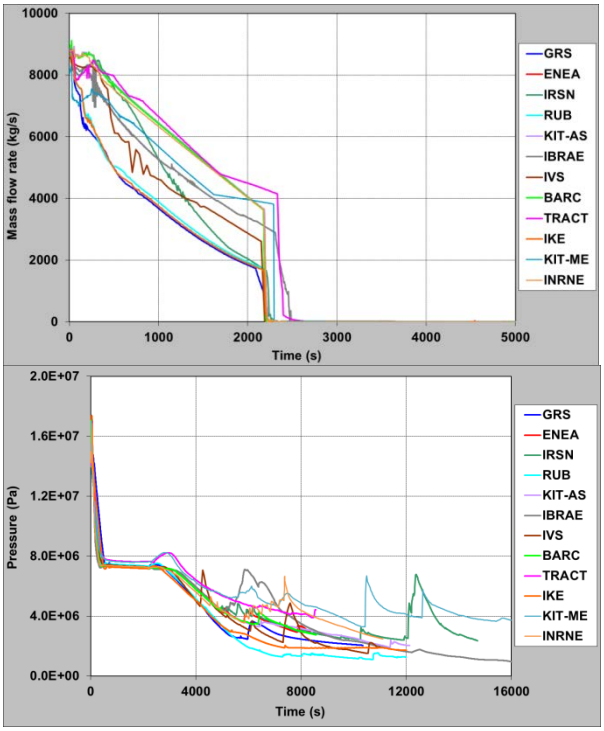

Figure 2: loop A mass flow rate (left) and pressurizer pressure (right)

The agreement in the onset of core heat-up is quite good among almost all calculations as shown by the time evolution of the fuel rod clad temperature at core top calculated in the central core channel is shown in Figure 3. The largest deviation is observed in the IRSN calculation with ICARE/CATHARE. This deviation is enhanced at the time of temperature escalation, likely due to 2D convective movements within the upper plenum of the vessel which are taken into account only with the ICARE/CATHARE code (however it is difficult to judge if the 2D upper plenum model gives more realistic results). The plot of clad temperature is stopped once degraded fuel rod relocation occurs at the top of the core, also due to transition to debris bed and collapse.

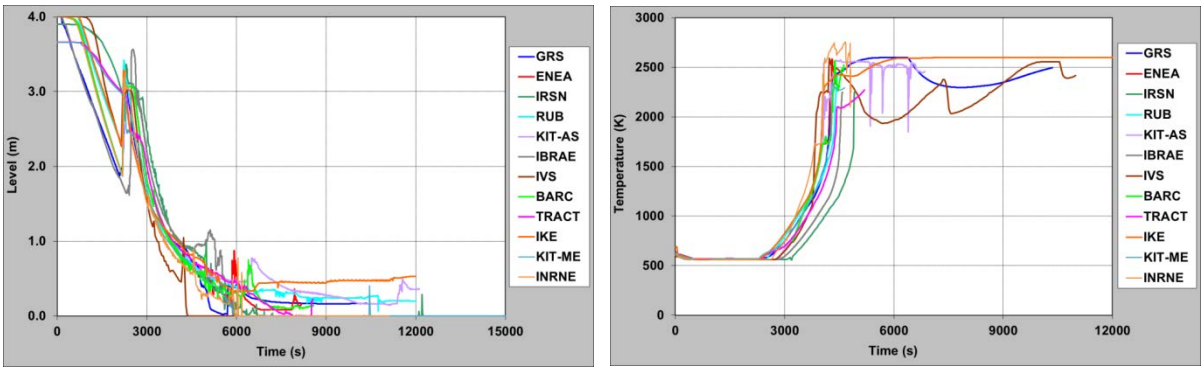

Figure 3: core collapsed level (left) and fuel rod clad temperature at core top (right)

The time evolution of instantaneous hydrogen generation and cumulative hydrogen production is compared in Figure 4. A large amount of hydrogen is predicted during the first oxidation phase in the period 4000 - 6000 s. Most of the participants calculate a similar amount of hydrogen at t = 6000 s in the range 300-380 kg. By this time, the lowest value of 218 kg is calculated with ICARE/CATHARE, likely due to delayed core heat-up induced by 2D convective movements, while a very high value near 750 kg is calculated with SOCRAT by IBRAE-RAS. Differently from all other codes, which rely on empirical parabolic correlations for zircaloy oxidation, the SOCRAT code is based on a more mechanistic model of oxidation diffusion kinetics, which could explain the large difference observed in cumulated hydrogen production. However, it is difficult to judge which model is more realistic. At the end of calculated transient (timing of vessel failure in most of the calculations), the cumulated hydrogen production spreads in the range 320 - 560 kg, except for SOCRAT code which calculates a much larger hydrogen mass close to 800 kg.

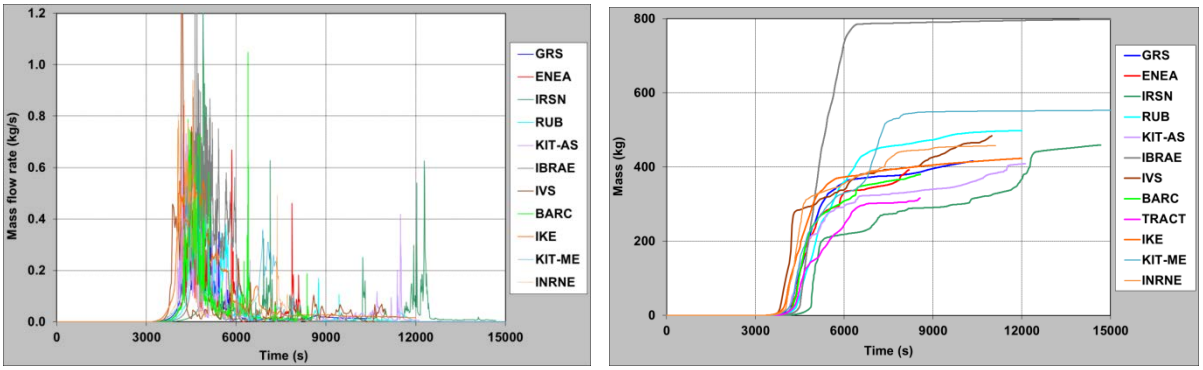

Figure 4: instantaneous hydrogen generation (left) and cumulated hydrogen production (right)

The time evolution of total mass of degraded core materials and of materials relocated in the lower plenum are compared in Figure 5. Core slumping in the lower plenum is not calculated by RUB and IKE with ATHLET-CD due to the lack of modelling in the code version used (stop of calculation at t = 12000 s without vessel failure). Other calculations stop at the time of vessel failure, while IRSN (ICARE/CATHARE), KIT (MELCOR) and IBRAE-RAS (SOCRAT) do not get as result any vessel failure due to large debris cooling in the lower head All codes agree on the onset of core degradation, but the total amount of degraded core materials spreads from 60 to 145 tons. There is also a significant spread in the timing of molten core slumping. Early vessel failure is predicted by Tractebel Engineering with MELCOR after core slumping due to vessel penetration failure which is not taken into account in all other calculations.

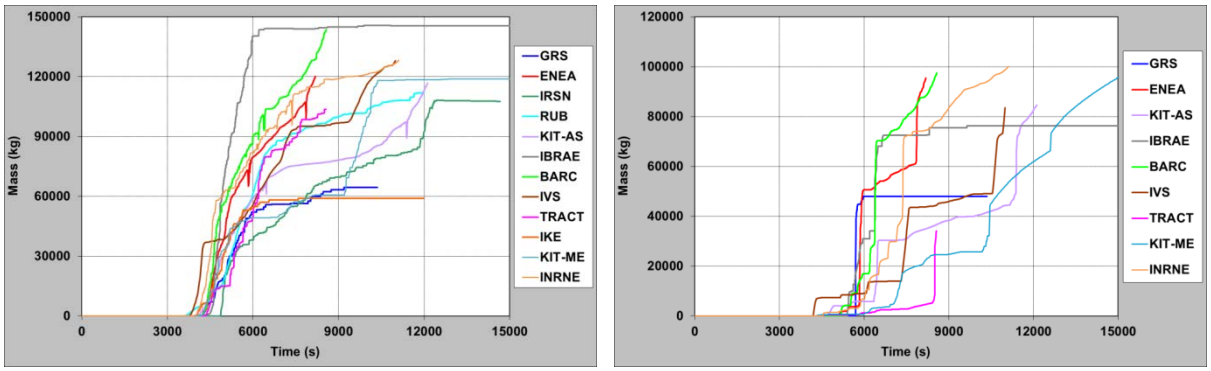

Figure 5: total mass of degraded core materials (left) and total mass of materials relocated in the lower plenum (right)

3.2.2 Reflooding start-up at 10 tons of degraded core materials

In all calculations the core reflooding is started when the total amount of degraded core materials reaches the value of 10 tons. This means that the reflooding is not started exactly at the same time but under similar core degradation conditions. The HPI reflooding rate was set to 25 kg/s that, including the make-up flow rate of 3 kg/s, corresponds to around 0.8 g/s of water per rod. As demonstrated by QUENCH experiments conducted at KIT, in general 1 g/s of water per rod would be sufficient to cooldown the core [3]. In the present case, a lower value is used (0.8 g/s) in order to investigate reflooding conditions at the limit of core coolability that seem the most challenging for the severe accident codes. All the calculations are stopped when the core heat-up and degradation progression is terminated by quenching, and then almost steady-state conditions are reached in the primary system.

The main results of this reflooding scenario are illustrated in Figures 6 to 8. Core reflooding starts at similar rate in all calculations between 4200 – 4800 s (Figure 6). The whole core covering is reached in about 1000 s. Only INRNE with ASTEC predicted a strong temperature escalation at core top up to 3000 K, because of a very high clad failure temperature limit (2700 K) used. Some of the participants predicted efficient quenching at core top, while in some of the calculations clad failure and relocation could not be avoided due to the limited reflooding rate.

Primary system refilling shown in Figure 7 is more or less consistent in all calculations. After around t = 7000 s, the primary coolant inventory remains almost constant, since the water injection by HPI and make-up systems is compensated by the increase of water-steam mixture leakage at the break. Significant primary pressure spikes are calculated by the codes at the onset of core reflooding (Figure 7), mainly due to strong thermal interaction between cold water and hot core structures, which induces large water vaporization.

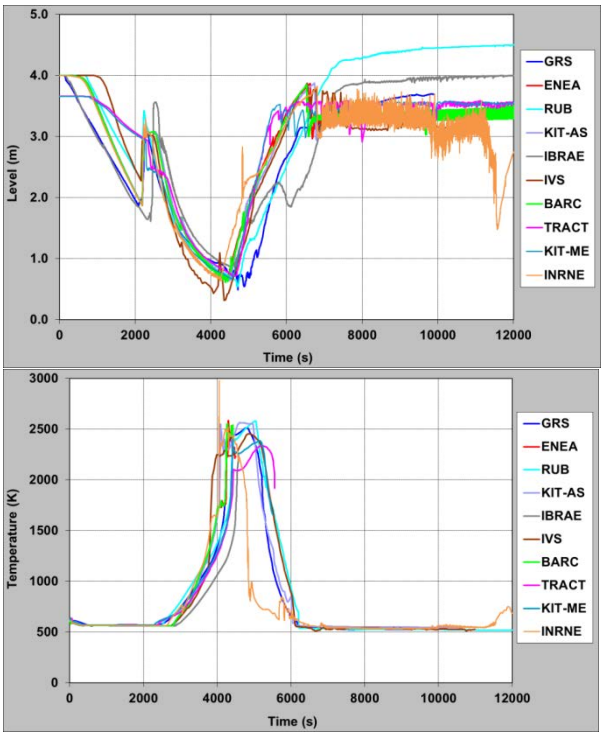

Figure 6: core collapsed level (left) and fuel rod clad temperature at core top (right)

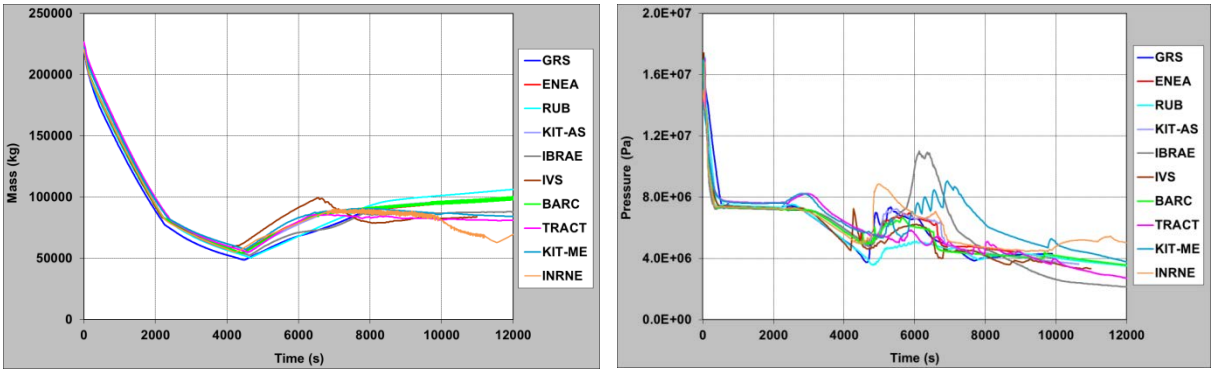

Figure 7: total primary mass (left) and pressurizer pressure (right)

The instantaneous and cumulated hydrogen production is shown in Figure 8. Following core quenching, some enhanced hydrogen peaks are calculated by the codes. However, in almost all calculations the hydrogen generation is stopped roughly after t = 6000 s due to efficient core structure cooldown. In most of the calculations, the hydrogen produced during reflooding is quite limited and seems mainly the result of delayed core quenching, instead of renewed oxidation of metallic materials following core structure collapse, melt formation and relocation. However, in case of SOCRAT calculation by IBRAE-RAS, the large mass of hydrogen generated is due to the oxidation of cladding melt. Magma oxidation is taken into account by the other codes, but the contribution to the total core oxidation seems much less important.

In all calculations, the core melt progression is terminated by core reflooding (Figure 9), but the timing is different and the total mass of degraded core materials spreads over a large range from 20 to 105 tons. The molten core slumping in the lower plenum is excluded or limited to a quite small amount, which prevents the vessel from failure in all calculations.

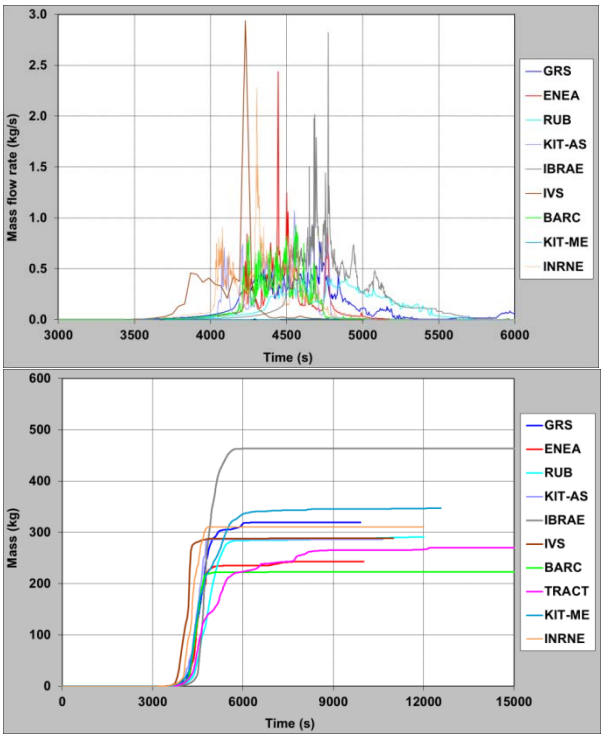

Figure 8: instantaneous hydrogen generation (left) and cumulated hydrogen production (right)

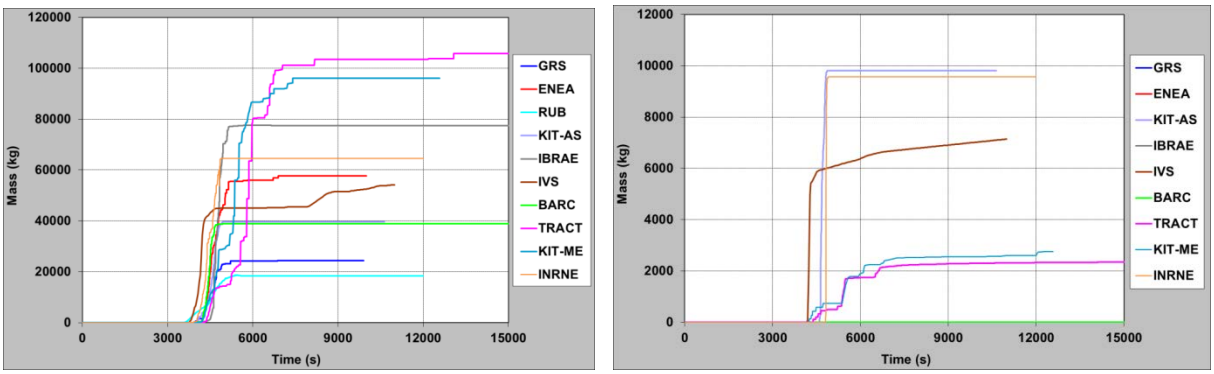

Figure 9: total mass of degraded core materials (left) and total mass of materials relocated in the lower plenum (right)

3.2.3 Reflooding start-up at 45 tons of degraded core materials

The only difference in this reflooding scenario with respect to the previous one is the extension of core degradation at the time of reflooding start-up. In fact, in this scenario the total mass of degraded core materials amounts to 45 tons instead of 10 tons. The main results of this reflooding scenario are shown in Figures 10 to 13.

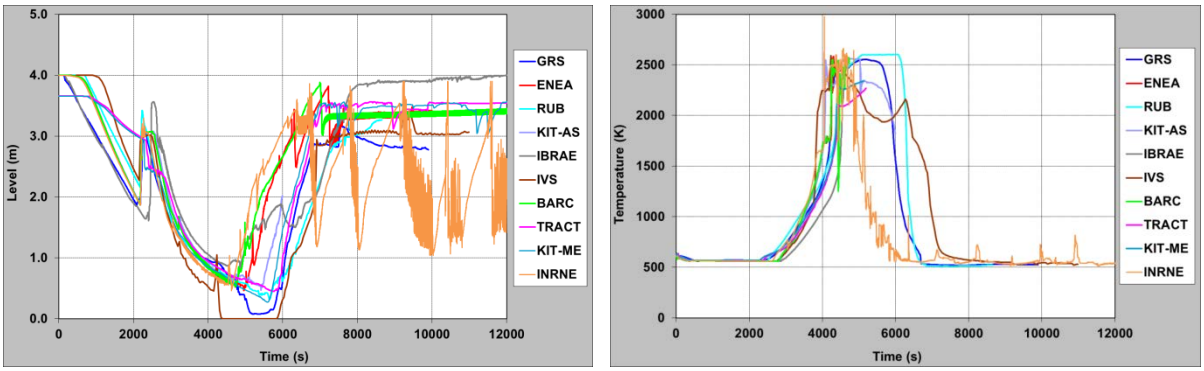

Figure 10: core collapsed level (left) and fuel rod clad temperature at core top (right)

In this case the onset of reflooding in all calculations is spread over a larger time interval because of the differences in core melt progression. The conclusions of the previous reflooding scenario apply as well in this case, regarding core quenching and cooldown rate (Figure 10), primary mass inventory and pressure behaviour (Figure 11). The hydrogen production (Figure 12) due to reflooding is still limited and stops in almost all calculations around 6000 – 7000 s, after complete core quenching. After this time, only MELCOR calculations by KIT and Tractebel Engineering show a continuous hydrogen production with progressive core melting (Figure 13), likely because the steam produced when corium slumps to the lower plenum might re-oxidize the remaining core. Also in this case the molten core slumping in the lower plenum is rather limited and then no vessel failure is predicted in the medium and long term in all calculations.

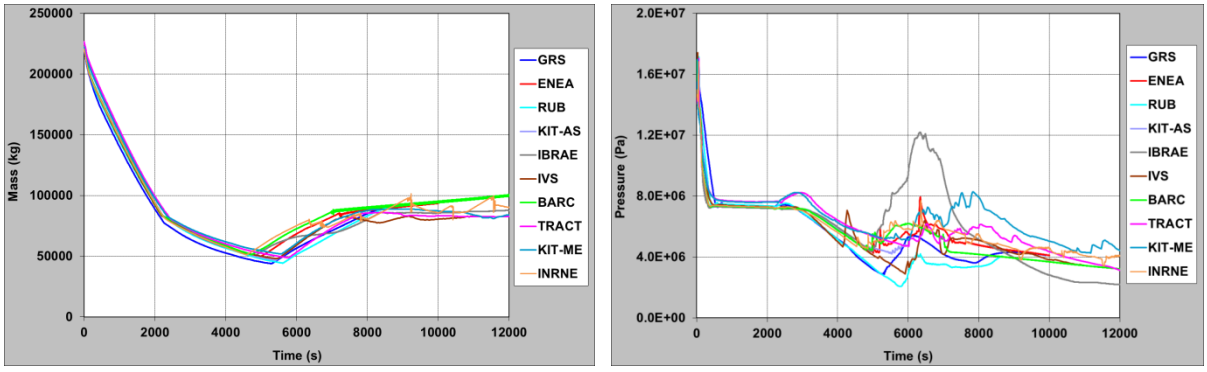

Figure 11: total primary mass (left) and pressurizer pressure (right)

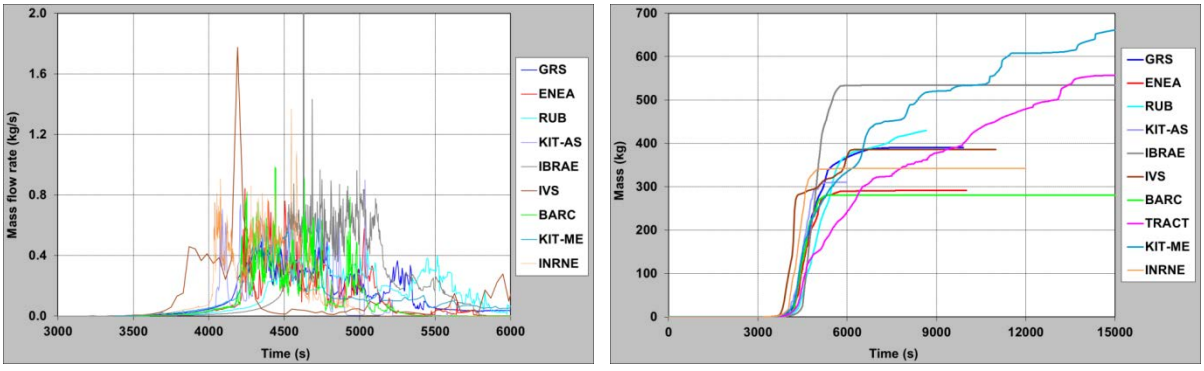

Figure 12: instantaneous hydrogen generation (left) and cumulated hydrogen production (right)

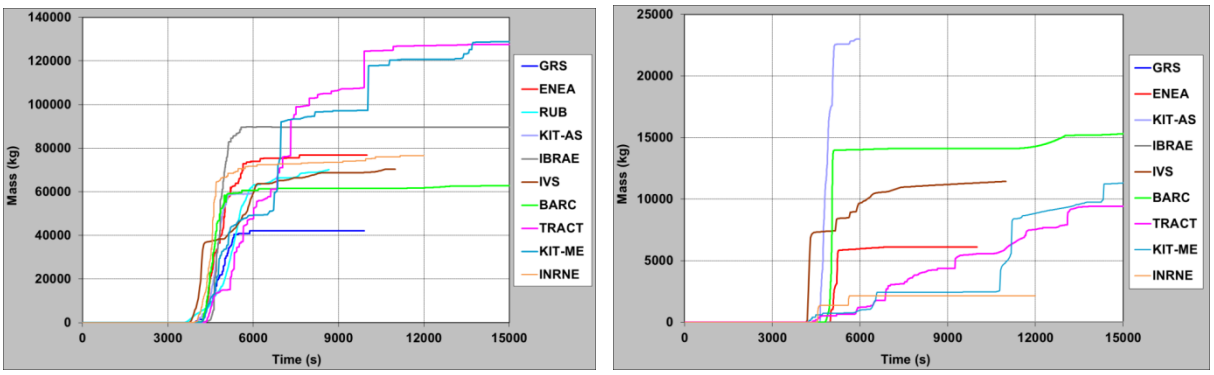

Figure 13: total mass of degraded core materials (left) and total mass of materials relocated in the lower plenum (right)

3.3 SLB sequence

In order to investigate a low pressure accident scenario, the double ended guillotine break (DEGB) of the surge line has been simulated in conjunction with the loss of offsite power supply (station blackout at t = 0 s). The loss of offsite power leads to immediate reactor scram, primary pump coastdown, and turbine and feedwater trip on the secondary side without auxiliary feedwater start-up. The large primary coolant leakage started by the surge line break leads to quick depressurization of the primary system with rapid primary coolant inventory depletion and consequent onset of core uncovery and heat-up.

As for the previous SBLOCA sequence, in the SLB base case calculation the HPI and LPI systems are not actuated and then the transient progressed until large core melting and slumping in the lower plenum with eventual vessel failure. Starting from the base case calculation, two reflooding scenarios have been defined with HPI actuation, starting from different core degradation conditions, as for the previous SBLOCA sequence.

A preliminary comparison of results for the SLB sequence analysis, including reflooding scenarios, is presented and briefly discussed in the following sub-sections. More wide and reliable comparison of SLB results will be undertaken once all revised participant contributions, based on more consistent boundary conditions and code model assumptions, will be submitted within the continuation of the benchmark activities after SARNET2. In particular, the preliminary calculation by KIT with MELCOR shows a very large delay in core heat-up, if compared to other code results, which needs to be verified.

3.3.1 Base case without reflooding

The aspects relevant to thermal-hydraulics in the primary system are illustrated in Figures 14 to 16. All the participants predicted a similar plant behaviour in the initial transient phase, which is characterized by fast primary system depressurization and coolant inventory depletion. However, some deviations in the prediction of the initial mass flow rate through the surge line break (Figure 14) contributed to enhance the differences observed in primary system pressure evolution (Figure 15), with relevant feedback on the break mass flow rate itself.

When the primary pressure approaches the containment pressure (a constant value of 1.5 bar is imposed as boundary condition in SLB calculations), after about t = 1000 s in most of the calculations, the break flow rate becomes negligible and the primary coolant mass remains almost constant (Figure 14). The residual coolant mass in the primary circuit varies, approximately, from 10 to 30 tons in the different code calculations. This deviation is of course reflected in the mass of water remaining in the lower plenum of the vessel and the loop seal of the cold legs.

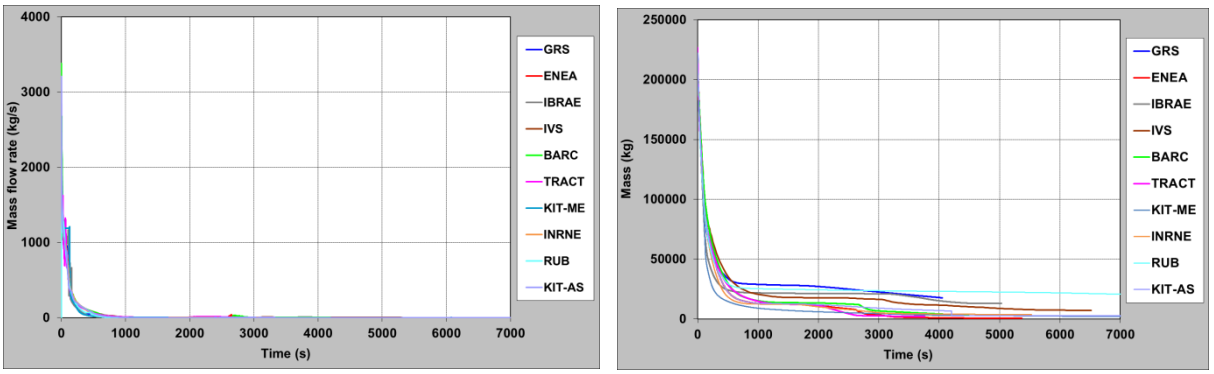

Figure 14: break flow rate (left) and total primary mass (right)

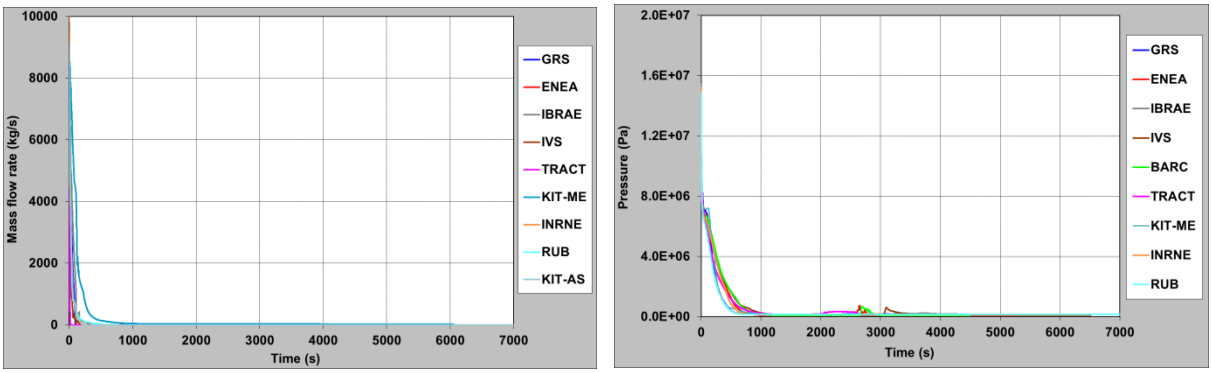

Figure 15: loop A mass flow rate (left) and vessel upper plenum pressure (right)

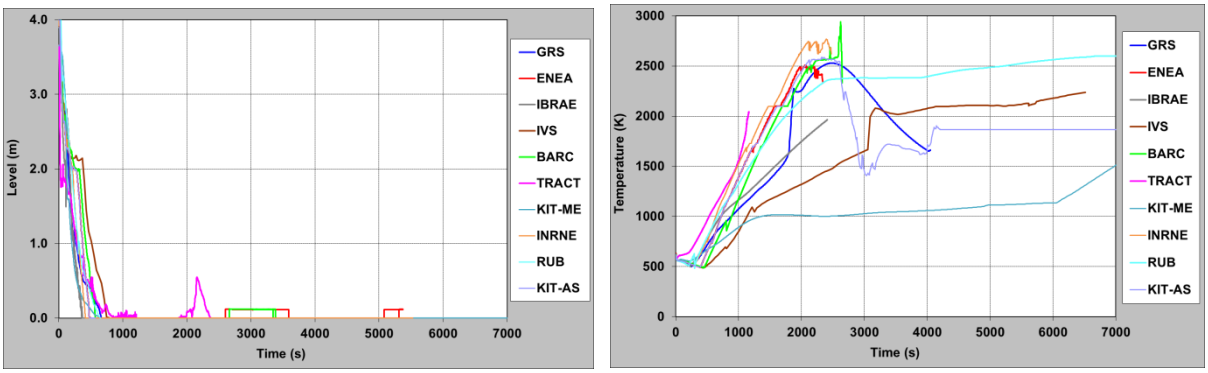

Figure 16: core collapsed level (left) and fuel rod clad temperature at core top (right)

All codes predict an early whole core uncovery in the time period 200 – 700 s (Figure 16). Because of early core uncovery, the fuel rod heat-up at the core top starts just few hundreds of seconds after transient initiation (the reason of the much delayed core heat-up calculated by KIT with MELCOR has yet to be clarified). An initial fuel rod heat-up rate as high as 1.7 K/s is calculated by the codes, according to the high decay power level of the initial transient phase.

Most of the participants did not calculate significant temperature excursions during the core heat-up phase since the oxidation of zircaloy claddings occurred under steam-starved conditions, owing to the limited availability of steam, once the collapsed water level falls down below the core bottom. This is also confirmed by the limited amount of hydrogen produced, as shown in Figure 17. Some temperature escalations, starting from about 1600 - 1700 K, observed in GRS and IVS calculations are likely produced by the enhancement of cladding oxidation, occurring when the steam availability sharply increases, following core material slumping and consequent strong molten jet/water thermal interaction in the lower plenum of the vessel.

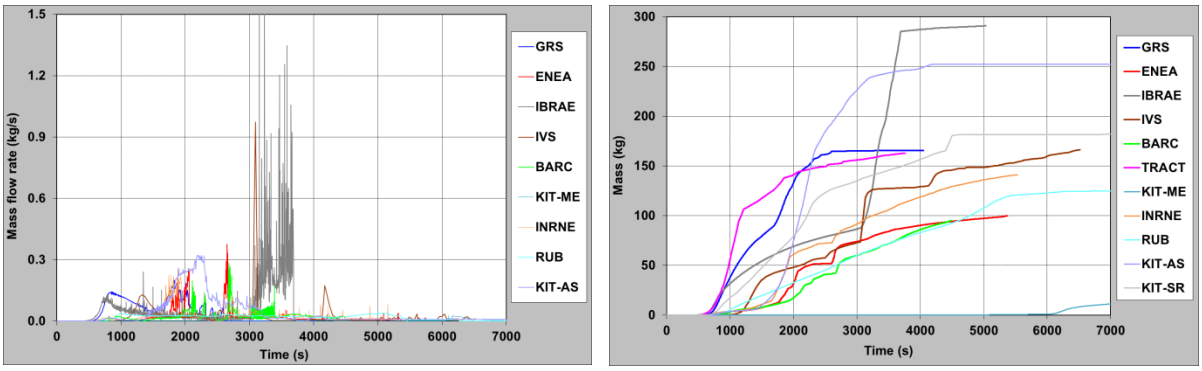

Figure 17: instantaneous hydrogen generation (left) and cumulated hydrogen production (right)

Although the timing of core degradation is somewhat different, almost all codes predict whole core damage during the transient phase with a total amount of degraded core materials, including melting of core support structures, in the range of 140 – 160 tons, as shown in Figure 18 for most calculations. The consequent material slumping into the lower plenum for these calculations is rather large: in the range of 110 – 140 tons. Only GRS and RUB with ATHLET-CD predict a much reduced core degradation and material slumping into the lower plenum. The ATHLET-CD version 2.2A used by RUB only allows to simulate one core relocation event which is assumed to start based on user-defined criteria, here when the degraded core mass reaches 60 tons, and then further core melt slumping cannot be taken into account. Differently, the ATHLET-CD version used by GRS (2.2 Cycle B) allows continuous material slumping into the lower plenum.

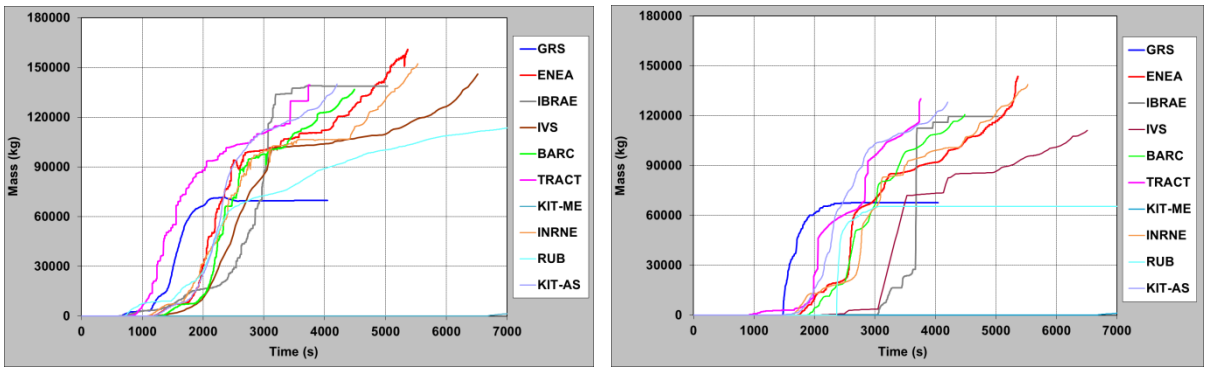

Figure 18: total mass of degraded core materials (left) and total mass of materials relocated in the lower plenum (right)

There is a quite large spreading on the timing of vessel failure (from t = 4000 s to t = 6500 s) which is calculated by all codes, because of the large amount of corium relocated in the lower head of the vessel and of the absence of water sources which may cool down the debris bed and molten pool materials.

The total amount of hydrogen produced ranges from 100 kg to 250 kg in different ASTEC calculations. In the ASTEC calculation by KIT, no debris bed (only magma) modelling is taken into account differently from ASTEC calculation by ENEA. This confirms that different late phase core degradation modelling can strongly impact on the hydrogen source and, at the same time, on core melt progression and corium relocation into the lower plenum.

3.3.2 Reflooding start-up at 10 tons of degraded core materials

As in case of SBLOCA reflooding scenario, the core reflooding is started when the total amount of degraded core materials reaches the value of 10 tons and the HPI reflooding rate was set to 28 kg/s.

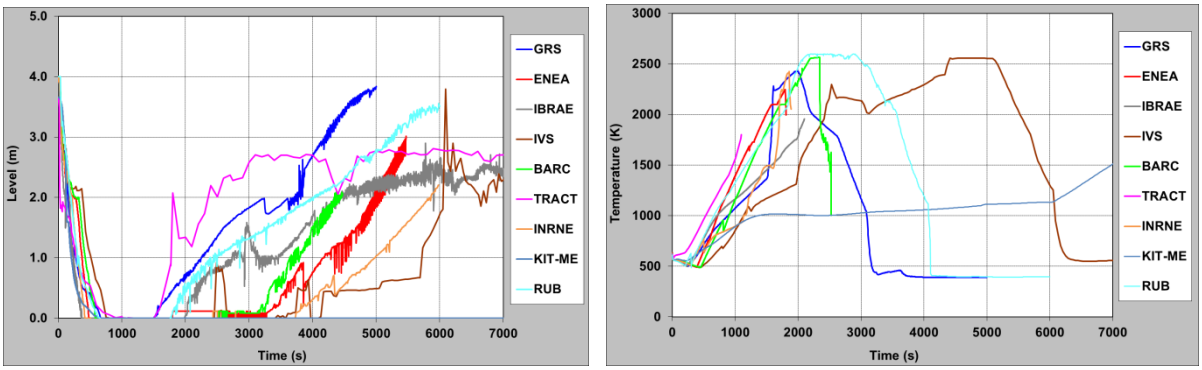

Figure 19: core collapsed level (left) and fuel rod clad temperature at core top (right)

The start of water collapsed level rise in the core (Figure 19), with consequent onset of core quenching, is delayed with respect to reflooding initiation, since the water collapsed level falls down below the core bottom before reflooding. Furthermore, the deviation in the timing of onset of core degradation contributes to enlarge the discrepancies observed in the time evolution of core collapsed water level calculated by the different codes.

In some calculations, the primary coolant mass increase is limited below 50 tons by renewed water-steam mixture leakage from the surge line break, while in some other calculations the primary coolant mass may increase up to about 90 tons (Figure 20).

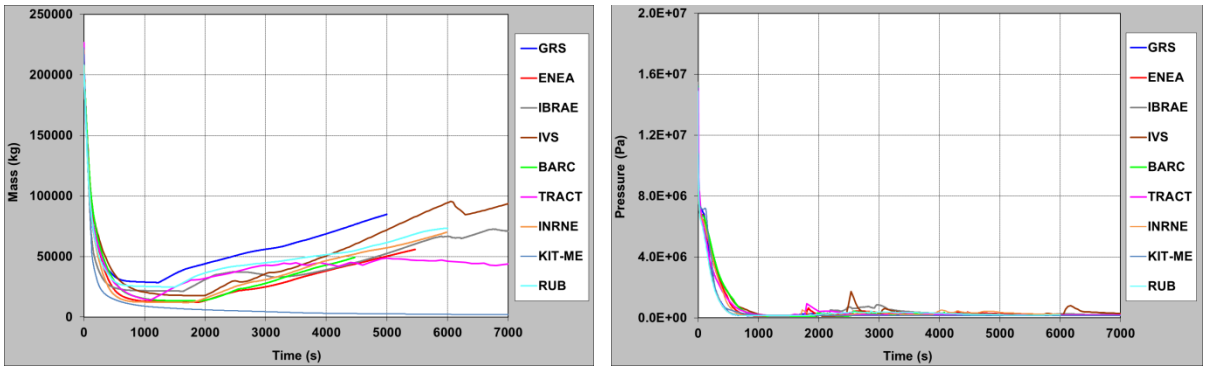

Figure 20: total primary mass (left) and vessel upper plenum pressure (right)

The hydrogen release during reflooding increases in almost all calculations with respect to the base case, due to the availability of steam provided by thermal interaction of water with hot core structures, but only two participants predicted very large hydrogen generation during core reflooding, as shown in Figure 21. The largest hydrogen mass of about 700 kg is calculated by RUB with ATHLET-CD where the transition to a debris bed is not modelled. Besides, up to 600 kg of hydrogen release is predicted by IBRAE-RAS with SOCRAT. In both calculations there was no significant material relocation into the lower plenum (see Figure 22) and thus, likely, a larger amount of metallic material remained in the core and oxidized during the reflooding phase.

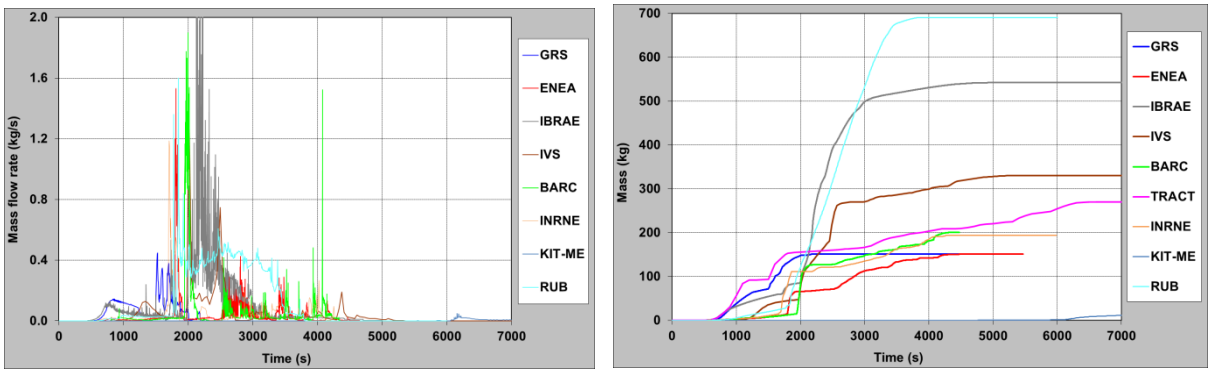

Figure 21: instantaneous hydrogen generation (left) and cumulated hydrogen production (right)

In some of the calculations, mainly ASTEC calculations, the slow core reflooding rate was not enough to cool the core and then to stop the core melt progression. As a consequence, in these calculations the whole core degradation and core material slumping into the lower plenum was not significantly limited and, therefore the vessel failure was only delayed by about 500 - 2000 s, with respect to the base case without reflooding. No vessel failure was predicted in this case by ATHLET-CD, MELCOR and SOCRAT codes due to the limited amount of materials relocated into the lower plenum or due to debris bed coolability in the lower head of the vessel filled by water.

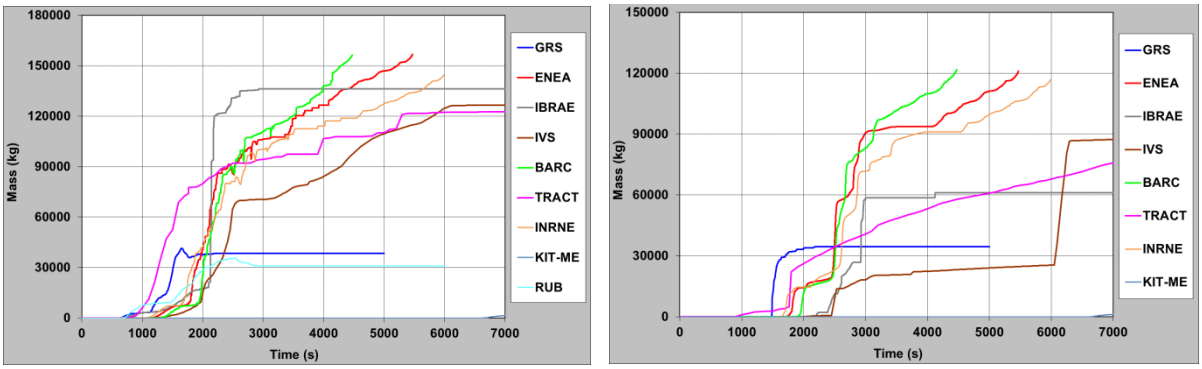

Figure 22: total mass of degraded core materials (left) and total mass of materials relocated in the lower plenum (right)

3.3.3 Reflooding start-up at 45 tons of degraded core materials

In this reflooding scenario the water injection by HPI, with a flow rate of 28 kg/s, is initiated as soon as the total mass of degraded core materials exceeds 45 tons. The comparison of code results is presented in Figures 23 to 26. Because of the further delay in core reflooding with respect to the previous reflooding scenario, in all calculations the core melt progression and core materials relocation into the lower plenum could not be significantly limited with respect to the base case. Furthermore, the hydrogen generation during core reflood was limited by early core materials slumping, and thus the additional hydrogen release due to reflooding was rather low in all calculations. As in the previous reflooding scenario, the vessel failure was just delayed in all ASTEC calculations, while no vessel failure was predicted in the other calculations mainly due to debris bed and molten pool coolability in the lower head of the vessel filled by water.

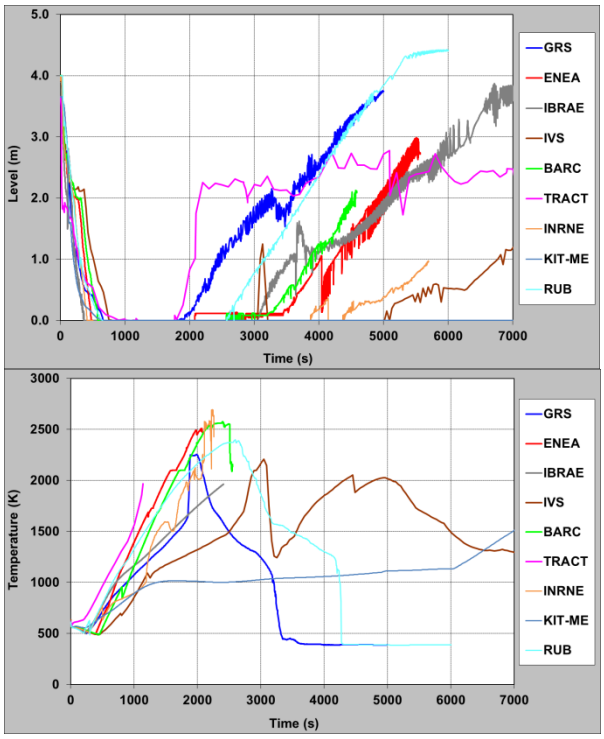

Figure 23: core collapsed level (left) and fuel rod clad temperature at core top (right)

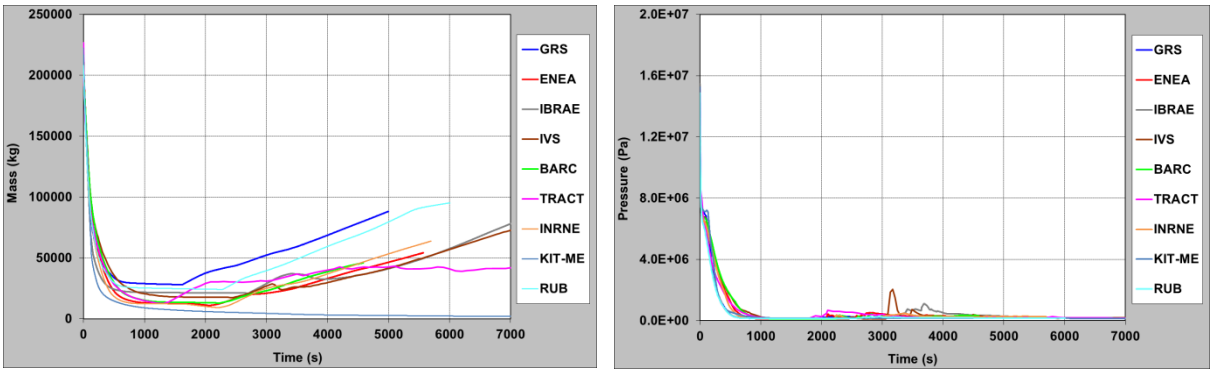

Figure 24: total primary mass (left) and vessel upper plenum pressure (right)

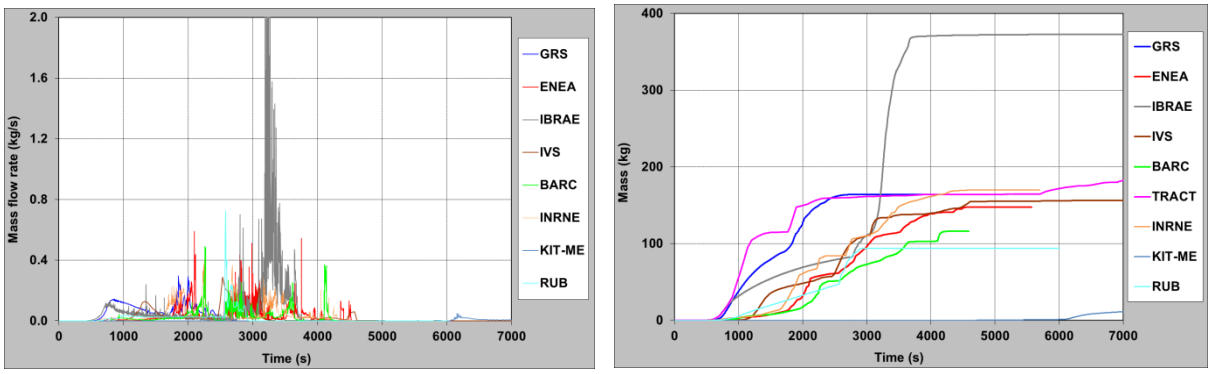

Figure 25: instantaneous hydrogen generation (left) and cumulated hydrogen production (right)

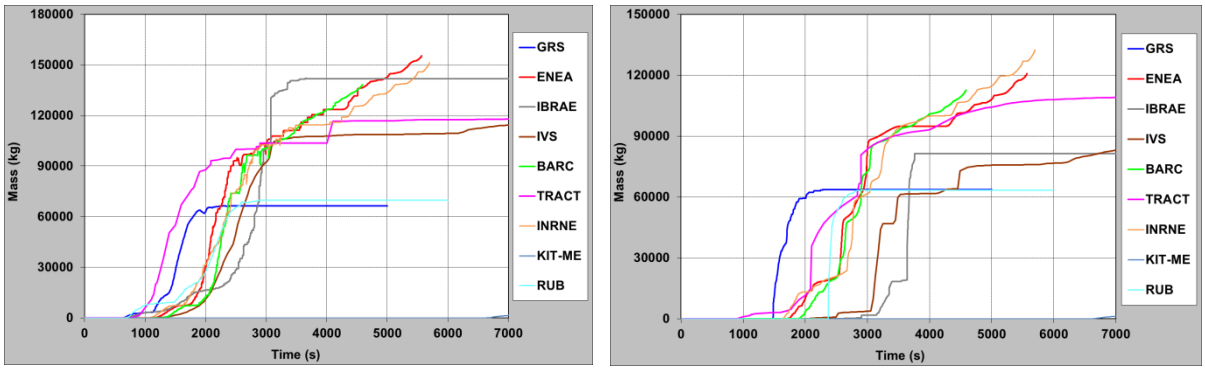

Figure 26: total mass of degraded core materials (left) and total mass of materials relocated in the lower plenum (right)

4 CONCLUSIONS

Within the current benchmark exercise on TMI-2 plant, SBLOCA and SLB sequences have been calculated by several organizations using different mechanistic and integral codes. Result comparison for the SBLOCA sequence and related reflooding scenarios have been presented and discussed in details, while the SLB sequence results presented are in a preliminary phase. The calculations confirm the general robustness of the codes. Indeed, all the codes were able to calculate the accident sequence up to the more severe degradation state and under degraded core reflooding conditions. While the uncertainties in the current code results seem not reduced with respect to the previous ATMI benchmark exercise [1], the present benchmark has highlighted the robustness of the codes for the analysis of the late phase degradation with core slumping into the lower head until vessel failure, thanks to the large effort spent by the code developers for physical modelling improvements in this field.

Thanks to the harmonisation of the initial steady-state and boundary conditions, the uncertainties on the prediction of the plant thermal-hydraulic behaviour have been minimized, at least before significant core degradation takes place. After important core melting and relocation, involving the loss of rod-like geometry, fuel rod collapse and debris bed, molten pool formation, the deviation in code results becomes more remarkable. This is primarily due to different core degradation models used by the codes, mainly in the late degradation phase. Furthermore, some differences in the plant and core discretization and in the value of core degradation parameters in input to the code might contribute to enhance the spread in the code results. These last effects are strictly connected with the user effect, and might be enhanced by the degree of freedom left by the code developers in the selection of code input parameter values. The importance of precise code user guidelines is strengthened, at least for reducing the difference between users of the same code. However, from the benchmark exercise it appears that the main reason for the extent of the results spread was not the user effect, but the difference in phenomenological modelling.

The preliminary code result comparison for the SLB sequence has highlighted the more challenging situation related to the calculation of this very fast transient due to larger uncertainties in the prediction of the break flow rate and then the whole primary system draining, which induce deviations in core uncovery and heat-up, core melt progression and hydrogen source.

The uncertainties on the calculation of reflooding scenarios are still rather large, especially in case of later core reflooding. In case of SBLOCA sequence, all codes predict more or less delayed core quenching without any significant core slumping into the lower plenum at the end of reflooding, which prevents the vessel from failure. Differently, in case of SLB sequence, slow and delayed core reflooding starting from degraded core with

relatively high density power has much reduced effectiveness for core quenching. Therefore, in most of the calculations, core melt progression and material slumping to the lower plenum cannot be terminated, and in some cases (ASTEC calculations) the vessel failure is not prevented.

REFERENCES

[1] F. Fichot, O. Marchand, G. Bandini, H. Austregesilo, M. Buck, M. Barnak, P. Matejovic, L. Humphries, K. Suh, S. Paci, Ability of Current Advanced Codes to Predict Core Degradation, Melt Progression and Reflooding - Benchmark Exercise on an Alternative TMI-2 Accident Scenario, NEA/CSNI/R(2009)3 (2009)

[2] K. N. Ivanov, T. M. Beam, A. J. Baratta, Pressurised Water Reactor Main Steam Line Break (MSLB) Benchmark, Volume 1: Final Specifications, NEA/NSC/DOC(99)8 (1999)

[3] W. Hering, C. Homann, Degraded Core Reflood: Present Knowlwdge Based On Experimental And Analytical Data, International Conference on Nuclear Energy for New Europe 2005, Bled, Slovenia, September 5-8, 2005